A&A, 686, A141 (2024)
https://doi.org/10.1051/0004-6361/202449321

Astronomy & Astrophysics

Is GN-z11 powered by a super-Eddington massive black hole?

Maulik Bhatt[1], Simona Gallerani[1], Andrea Ferrara[1], Chiara Mazzucchelli[2], Valentina D'Odorico[1,3,4], Milena Valentini[3,5,6], Tommaso Zana[7], Emanuele Paolo Farina[8], and Srija Chakraborty[1]

[1] Scuola Normale Superiore, Piazza dei Cavalieri 7, 56126 Pisa, Italy
e-mail: maulik.bhatt@sns.it
[2] Instituto de Estudios Astrofísicos, Facultad de Ingeniería y Ciencias, Universidad Diego Portales, Avenida Ejercito Libertador 441, Santiago, Chile
[3] INAF – Osservatorio Astronomico di Trieste, via Tiepolo 11, 34131 Trieste, Italy
[4] IFPU – Institute for Fundamental Physics of the Universe, Via Beirut 2, 34014 Trieste, Italy
[5] Astronomy Unit, Department of Physics, University of Trieste, via Tiepolo 11, 34131 Trieste, Italy
[6] ICSC – Italian Research Center on High Performance Computing, Big Data and Quantum Computing, Italy
[7] Dipartimento di Fisica, Sapienza, Università di Roma, Piazzale Aldo Moro 5, 00185 Roma, Italy
[8] Gemini Observatory, NSF's NOIRLab, 670 N A'ohoku Place, Hilo, Hawai'i 96720, USA

Received 23 January 2024 / Accepted 7 March 2024

ABSTRACT

Context. Observations of $z \sim 6$ quasars powered by supermassive black holes (SMBHs; $M_{\rm BH} \sim 10^{8-10}\,M_\odot$) challenge our current understanding of early black hole (BH) formation and evolution. The advent of the *James Webb* Space Telescope (JWST) has enabled the study of massive BHs (MBHs; $M_{\rm BH} \sim 10^{6-7}\,M_\odot$) up to $z \sim 11$, thus bridging the properties of $z \sim 6$ quasars to their ancestors.
Aims. The JWST spectroscopic observations of GN-z11, a well-known $z = 10.6$ star-forming galaxy, have been interpreted with the presence of a super-Eddington (Eddington ratio $\equiv \lambda_{\rm Edd} \sim 5.5$) accreting MBH. To test this hypothesis, we used a zoom-in cosmological simulation of galaxy formation and BH co-evolution.
Methods. We first tested the simulation results against the observed probability distribution function (PDF) of $\lambda_{\rm Edd}$ found in $z \sim 6$ quasars. Then, in the simulation we selected the BHs that satisfy the following criteria: (a) $10 < z < 11$, (b) $M_{\rm BH} > 10^6\,M_\odot$. Next, we applied the extreme value statistics to the PDF of $\lambda_{\rm Edd}$ resulting from the simulation.
Results. We find that the probability of observing a $z \sim 10{-}11$ MBH accreting with $\lambda_{\rm Edd} \sim 5.5$ in the volume surveyed by JWST is very low (<0.2%). We compared our predictions with those in the literature, and discussed the main limitations of our work.
Conclusions. Our simulation cannot explain the JWST observations of GN-z11. This might be due to: (i) poor resolution and statistics in simulations, (ii) simplistic sub-grid models (e.g. BH accretion and seeding), (iii) uncertainties in the data analysis and interpretation.

Key words. galaxies: high-redshift – quasars: general – quasars: supermassive black holes

1. Introduction

Observations have shown that the most distant quasars known so far (redshift $z = 6{-}7.5$; see a recent review by Fan et al. 2023) are powered by supermassive black holes (SMBHs) with masses $\sim 10^{8-10}\,M_\odot$ (e.g. Bañados et al. 2018; Yang et al. 2020, 2023; Wang et al. 2021; Farina et al. 2022; Mazzucchelli et al. 2023). The existence of these gigantic black holes (BHs) presents a puzzle for current theoretical models of BH formation and evolution that is still lacking several pieces, for example, knowledge about the SMBH seed nature and mass and their ability to grow fast enough to assemble an SMBH in less than 1 Gyr, the age of the Universe at $z \sim 6$. Studying massive black holes (MBHs) of $\sim 10^{6-7}\,M_\odot$ at redshift $z > 9$ is essential in order to take a step forward in this field (Inayoshi et al. 2020; Volonteri & Bellovary 2012).

The most recent *James Webb* Space Telescope (JWST) observations have revealed the presence of accreting ($L_{\rm bol} \sim 10^{44-47}\,L_\odot$) MBHs in galaxies up to $z \sim 10{-}11$ (e.g. Bosman et al. 2023; Greene et al. 2024; Goulding et al. 2023; Furtak et al. 2024; Kokorev et al. 2023; Larson et al. 2023; Maiolino et al. 2024). These data are powerful tools for constraining different seeding scenarios (e.g. Jeon et al. 2024; Trinca et al. 2022, 2024; Pacucci et al. 2023; Schneider et al. 2023). A lot of interest in particular has been aroused by the detection of a vigorously accreting MBH in GN-z11, a well-known star-forming galaxy at $z = 10.6$ (Maiolino et al. 2024).

The galaxy GN-z11 was first identified by Bouwens et al. (2010) and Oesch et al. (2016). Recently, the JWST Advanced Deep Extragalactic Survey (JADES; Eisenstein et al. 2023) provided follow-up observations by means of NIRSpec spectroscopy (Bunker et al. 2023) and NIRCam imaging (Tacchella et al. 2023). These observations suggest that GN-z11 is an active galactic nucleus (AGN). The evidences in favour of this interpretation include the followings (Maiolino et al. 2024): (i) high ionisation transitions (e.g. [NeIV]λ2422, 2244), which are commonly observed in AGN (Terao et al. 2022; Le Fèvre et al. 2019) and are considered as tracers of AGN activity since they require high photon energies ($E_\nu > 63.5\,$eV) that are not easily produced by stars; (ii) NIII] multiplet, indicating gas densities ($>10^{10}\,{\rm cm^{-3}}$) typically found in the broad-line regions (BLRs) of AGN; (iii) a very deep equivalent width (${\rm EW_{rest}} \sim 5\,$Å) and a blueshifted absorption trough of a CIV doublet, suggesting the presence of outflows with velocities ($\sim 800{-}1000\,{\rm km\,s^{-1}}$) commonly observed in mini-broad absorption line (BAL) quasars (Rodríguez Hidalgo 2009); (iv) a

potentially broad profile of the HeIIλ1640 line that could come from the inner region of the BLR but could also trace the presence of a Wolf–Rayet (WR) stellar population; (v) clear detection of an MgII doublet hinting at the presence of an accreting MBH with mass $\sim 1.2 \times 10^6\, M_\odot$ and a surprisingly large Eddington ratio ($\lambda_{\rm Edd} = L_{\rm bol}/L_{\rm Edd} \sim 5.5 \pm 2$).

The high-accretion rate of GN-z11 provides important constraints for theoretical models predicting the mass and the formation epoch of early SMBH seeds (Inayoshi et al. 2020; Volonteri et al. 2021; Latif & Ferrara 2016). The various possibilities include: (1) light seeds ($\sim 10^{1-2}\, M_\odot$) from Pop III stars ($z \sim 20-30$, Madau & Rees 2001); (2) intermediate seeds ($\sim 10^{3-4}\, M_\odot$) from the collapse of supermassive stars or runaway collisions in dense nuclear star clusters; ($z \sim 10-20$, Devecchi et al. 2012; Greene et al. 2020; Kroupa et al. 2020) (3) heavy seeds ($\sim 10^{5-6}\, M_\odot$) produced by the collapse of metal-free gas in atomic-cooling (virial temperature $T_{\rm vir} > 10^4$ K) halos exposed to a strong Lyman-Werner radiation ($z \sim 10-20$), the so-called direct collapse BHs (DCBHs; Ferrara et al. 2014; Haehnelt & Rees 1993; Mayer & Bonoli 2019).

Of the above scenarios, the most favourable to explain the existence of SMBHs at high-z is still unclear. On the one hand, the DCBH scenario has the advantage that heavy seeds can grow at a mild pace, namely at sub-Eddington rates ($f_{\rm Edd} = \dot{M}/\dot{M}_{\rm Edd} < 1$). However, the conditions for the formation of DCBH are not easily satisfied. On the other hand, light/intermediate seeds can form in less extreme circumstances, but they require sustained ($f_{\rm Edd} > 1$) accretion rates for prolonged (~Gyr) intervals of time. Recent observations of $10^{7-8}\, M_\odot$ BHs at $z \sim 7-8$ (e.g. Larson et al. 2023; Kokorev et al. 2023) can be explained with both scenarios. The observed properties of GN-z11 can be reproduced by super-Eddington slim-disc accreting BHs descending from light and heavy seeds (Schneider et al. 2023); the more extreme case of UHZ-1 at $z \sim 10$ (Goulding et al. 2023) lends support to the heavy seeding channel.

Semi-analytical works that support light seed scenarios are based on radiatively inefficient "slim-disc" models in which super- or hyper-Eddington accretion (Sądowski 2009) can occur (e.g. Madau et al. 2014; Pezzulli et al. 2016, 2017; Trinca et al. 2022). However, it is still not completely understood how much these results depend on the assumptions adopted. To start with, Madau et al. (2014) assumed that, in super- or hyper-Eddington accretion regimes, gas can flow towards the centre BH almost non-affected by feedback processes. However, radiative feedback in radiatively efficient "thin disk" models (e.g. Pacucci & Ferrara 2015; Orofino et al. 2018) has been shown to modify the accretion flow onto the BH, either decreasing the accretion to sub-Eddington rates or making $f_{\rm Edd} > 1$ episodes intermittent. In particular, Pacucci et al. (2017) have shown that very efficient and prolonged large accretion rates only occur in $M_{\rm BH} > 10^4\, M_\odot$. For what concerns the Pezzulli et al. (2017) results, the adoption of $f_{\rm Edd} > 500$ values, which goes beyond the applicability of the adopted "slim-disc" recipe, may overestimate the accretion rate of light seeds and therefore the final mass of the formed SMBH.

The hydrodynamical simulations developed so far have provided further important information about this issue. Lupi et al. (2016) produced high-resolution (<1 pc) simulations of an isolated disc in which the radiatively inefficient supercritical accretion of light seeds occurs in the high density environment of gaseous circumnuclear discs. These authors find that $10-100\, M_\odot$ BHs can increase their mass within a few million years by between one and up to three orders of magnitude, depending on the resolution adopted (the higher the resolution, the lower the final mass of the grown seed). Less efficient growth of light seeds has been found by Smith et al. (2018), who followed the evolution of Bondi accreting BHs from Pop III stars in high-resolution cosmological simulations, finding a much smaller (<10% of their initial mass) average mass increase. Similar conclusions have been drawn by a comprehensive study performed by Zhu et al. (2022), who considered various recipes for BH seeding, accretion models, and feedback processes. Even in the most optimistic conditions (radiatively inefficient, super Eddington accretion) and despite spending a substantial fraction of time (~100 Myr) in super-critical accretion, light seeds ($M < 10^3\, M_\odot$) cannot reproduce $>10^7\, M_\odot$ ($>10^5\, M_\odot$) BHs at $z \sim 6$ ($z \sim 11$).

Current investigations have not definitively clarified whether light seeds can provide a valuable route for the formation of high-z MBHs. Furthermore, high-resolution (computationally expensive) hydrodynamical simulations are required to properly follow the growth of light seeds. Several works (see Table 1 in Habouzit et al. 2021) have thus opted to assume the DCBH scenario as a seeding prescription. In this work, we adopted the cosmological zoom-in hydrodynamical simulations developed by Valentini et al. (2021, hereafter V21). These simulations can reproduce the main properties of the most luminous $z \sim 6$ quasars (see Tables 2 and 3 in V21), namely the mass of their central SMBHs ($\sim 10^9\, M_\odot$) suggested by observations of the CIV and MgII lines (e.g. Farina et al. 2022; Mazzucchelli et al. 2023), their high star formation rates (SFRs; i.e. $\sim 100\, M_\odot\, {\rm yr}^{-1}$), and their large masses ($\sim 10^9\, M_\odot$) of molecular gas suggested by ALMA observations (e.g. Wang et al. 2016; Venemans et al. 2017, 2020; Gallerani et al. 2017; Decarli et al. 2018, 2022). In this work, we investigate the predictions of V21 simulations in terms of the accretion properties that characterise $z \sim 10-11$ BHs as massive as the one hosted in GN-z11 ($M_{\rm BH} \gtrsim 10^6\, M_\odot$).

In particular, to test whether the V21 simulations can reproduce the $\lambda_{\rm Edd} \sim 5.5$ found in GN-z11, we adopted the extreme value statistics (EVS; Gumbel 1958; Kotz & Nadarajah 2000). The EVS have been applied to a wide range of topics in cosmology (Lovell et al. 2023; Harrison & Coles 2011; Colombi et al. 2011; Chongchitnan & Silk 2012; Davis et al. 2011; Waizmann et al. 2011; Mikelsons et al. 2009; Chongchitnan & Silk 2021) and can be used to calculate the probability of randomly extracting the largest (or smallest) value from an underlying distribution.

This paper is organised as follows: In Sect. 2, we describe the adopted numerical simulations. We then test the accretion model adopted in our simulations in Sect. 3 by comparing the simulated Eddington ratio probability distribution function (PDF) with the largest sample of sources for which this quantity has been measured so far. In Sect. 4, we compute the exact EVS PDF of the Eddington ratio for GN-z11-like MBH from the simulations. Finally, we discuss our results and draw our conclusions in Sect. 5. Throughout the paper we have considered a flat ΛCDM cosmology with the following cosmological parameter values: baryon density $\Omega_{\rm b}\, h^2 = 0.0224$, DM density $\Omega_{\rm dm}\, h^2 = 0.12$, Hubble constant $H_0 = 67.74\, {\rm km\, s^{-1}\, Mpc^{-1}} = 100\, h$, and the late-time fluctuation amplitude parameter $\sigma_8 = 0.826$ (Planck Collaboration VI 2020).

2. Simulations

We used the hydrodynamical cosmological zoom-in simulations developed by V21. We summarise the main features of this model below. In particular, we considered the AGN fiducial run featuring thermal AGN feedback as our fiducial model, and we refer the reader to V21 for more details. The V21 simulation

adopted in this work was performed with a non-public version of the TreePM (particle mesh) and SPH (smoothed particle hydrodynamics) code GADGET-3 (Valentini et al. 2017, 2019, 2020), an upgraded version of the public GADGET-2 code (Springel 2005).

2.1. Initial conditions and resolution

The software MUSIC[1] Hahn & Abel (2011) was used to generate the initial conditions, assuming a ΛCDM cosmology. First, a dark matter (DM)-only simulation with a mass resolution of DM particles of $9.4 \times 10^8\ M_\odot$ in a comoving volume of $(148\,\mathrm{Mpc})^3$ was run starting from $z = 100$ down to $z = 6$. Then, a halo as massive as $M_{\rm halo} = 1.12 \times 10^{12}\ M_\odot$ at $z = 6$ was selected for a zoom-in procedure in order to run the full hydrodynamical simulation. In the zoom-in region, the highest resolution particles have a mass of $m_{\rm DM} = 1.55 \times 10^6\ M_\odot$ and $m_{\rm gas} = 2.89 \times 10^5\ M_\odot$. The gravitational softening lengths are[2] $\epsilon_{\rm DM} = 0.72$ ckpc and $\epsilon_{\rm bar} = 0.41$ ckpc for the DM and the baryon particles, respectively.

2.2. Sub-resolution physics

2.2.1. Black hole seeding

The DM halos exceeding the threshold mass $M_{\rm DM} = 1.48 \times 10^9\ M_\odot$ were seeded with a BH of mass $M_{\rm BH,seed} = 1.48 \times 10^5\ M_\odot$ if no BH was already seeded in previous time steps. This value of seed mass mimics the DCBH scenario.

2.2.2. Black hole growth

Black holes grow due to gas accretion and merger with other BHs. The gas accretion was modelled assuming a Bondi–Hoyle–Lyttleton accretion solution (Bondi 1952; Hoyle & Lyttleton 1939; Bondi & Hoyle 1944):

$$\dot{M}_{\rm bondi} = \frac{4\pi G^2 M_{\rm BH}^2 \langle \rho_{\rm gas} \rangle}{(\langle c_{\rm s} \rangle^2 + \langle v_{\rm BH} \rangle^2)^{3/2}}, \tag{1}$$

where $M_{\rm BH}$ is the mass of the BH, $\rho_{\rm gas}$ is the gas density, G is the gravitational constant, $c_{\rm s}$ is the sound speed, and $v_{\rm BH}$ is the velocity of the BH relative to the gas. All the quantities of the gas particles are calculated within the BH smoothing length using kernel-weighted contributions. The BH accretion rate was capped to the Eddington value. A small fraction, $\epsilon_{\rm r}\ \dot{M}_{\rm accr}$, of the accreted mass is converted into radiation; thus, the actual growth rate of the BH mass can be written as

$$\dot{M}_{\rm BH} = (1 - \epsilon_{\rm r})\ \dot{M}_{\rm accr}, \tag{2}$$

where $\epsilon_r = 0.03$ is the radiation efficiency (Sądowski & Gaspari 2017). The BHs instantaneously merged if their distance became smaller than twice their gravitational smoothing length and if their relative velocity was smaller than $0.5\ c_{\rm s}$ ($v_{\rm BH-BH} < 0.5\ \langle c_{\rm s} \rangle$). The position of the resulting BH is the position of the most massive one between the two progenitor BHs.

2.2.3. Active galactic nucleus feedback

For what concerns AGN feedback, a fraction $\epsilon_{\rm f}$ of the bolometric luminosity $L_{\rm bol} = \epsilon_{\rm r} \dot{M}_{\rm BH} c^2$ is distributed to the gas particles thermally and isotropically within the BH smoothing volume (Valentini et al. 2020). V21 adopt $\epsilon_{\rm f} = 10^{-4}$, tuned to match the normalisation of the black hole to stellar mass relation at $z = 6$.

3. Eddington ratio predictions against $z \sim 6$ data

In this section, we compare the Eddington ratios $\lambda_{\rm Edd}$ measured for $z \sim 6$–7.5 quasars with the results from the V21 simulation. The Eddington ratio is defined as $\lambda_{\rm Edd} = L_{\rm bol}/L_{\rm Edd}$, namely the ratio between the bolometric luminosity of a quasar and its Eddington luminosity that, under the assumption of hydrostatic equilibrium and pure ionised hydrogen, can be written as (Eddington 1926)

$$L_{\rm Edd} = \frac{4\pi G\ M_{\rm BH}\ m_{\rm p}\ c}{\sigma_{\rm T}}, \tag{3}$$

where $m_{\rm p}$ is the mass of a proton and $\sigma_{\rm T}$ is the Thomson scattering cross-section.

For what concerns the observed $\lambda_{\rm Edd}$ values, we considered both the sample of 38 quasars by Farina et al. (2022, hereafter F22) and the sample of 42 quasars by Mazzucchelli et al. (2023, hereafter M23), the latter includes the XQR-30 sample of VLT-Xshooter observations (D'Odorico et al. 2023). Of the 80 quasars in the combined sample, 18 of them are present in both samples. In these cases, we considered the data characterised by the smallest error. After removing duplicates, we had 62 bright quasars at $5.8 < z < 7.5$. Hereafter, we refer to this combined sample as the "literature sample".

F22 and M23 provide the $\lambda_{\rm Edd}$ values resulting from the analysis of the MgII and CIV emission lines using different methods (MgII line: Vestergaard & Osmer 2009; Shen et al. 2011; CIV line: Vestergaard & Peterson 2006; Coatman et al. 2017). When the MgII line was available, we used the Shen et al. (2011) method since it provides the smallest errors (see also Shen & Liu 2012, for a comparison among different virial BH mass estimators). For the targets in which only the CIV line fit is provided, we adopted the Vestergaard & Peterson (2006) method. The resulting "observed" PDF of the $\lambda_{\rm Edd}$ values is shown in the left panel of Fig. 1, indicated with the orange shaded region[3].

To compute $\lambda_{\rm Edd}$ values from V21 simulation, we considered the accretion rate of the SMBHs that have masses consistent with the literature sample (namely $M_{\rm BH} > 10^8\ M_\odot$) in the redshift range $6 < z < 7.5$. We ended up with two SMBHs that satisfy these criteria. We finally selected the SMBH with $L_{\rm bol} > 2.7 \times 10^{46}\ L_\odot$. This choice enables a proper comparison between observations and simulation since the observed sample consists of very luminous quasars (the least luminous source has $L_{\rm bol} = 2.86^{+0.17}_{-0.15} \times 10^{46}\ L_\odot$). We evaluated $\lambda_{\rm Edd}$ for the selected BH[4] at each time step of the simulation in the redshift range $6 < z < 7.5$. We considered each accretion episode as independent and computed the corresponding PDF. The resulting "simulated" PDF is shown in the left panel of Fig. 1 with a blue shaded region.

From the comparison between the observed and simulated PDF, it resulted that the median of these distributions (0.46 for the observed PDF and 0.44 for the simulated one) are perfectly consistent with each other (see the vertical orange and blue lines

[1] MUSIC stands for Multiscale Initial Conditions for Cosmological Simulations: https://bitbucket.org/ohahn/music

[2] A letter c before the corresponding unit refers to comoving distances (e.g. ckpc).

[3] M23 used bolometric correction by Richards et al. (2006) to calculate $L_{\rm bol}$. These bolometric corrections were found to overestimate $L_{\rm bol}$ in the case of highly luminous quasars (Trakhtenbrot & Netzer 2012). Thus, the actual PDF of $\lambda_{\rm Edd}$ may be shifted towards lower values.

[4] This is the BH located at the centre of the most massive sub-halo. Further properties of this BH have been thoroughly analysed in V21.

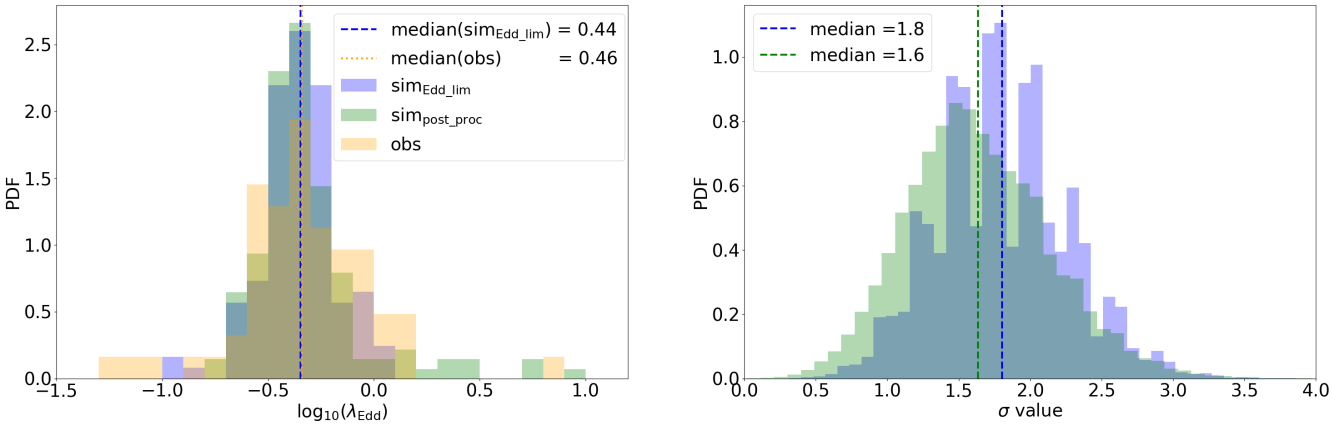

Fig. 1. Comparison between observations of $z \sim 6$ quasars and simulations. Left panel: the orange histogram shows the probability distribution function of Eddington ratios measured from the literature sample of quasars at $6 < z < 7.5$. This is compared with Eddington ratio values obtained from the Eddington-limited accretion model (V21; blue histogram), and with Eddington ratio values obtained in post processing from V21 using Eq. (1) (green histogram). Right panel: distribution of the σ values obtained by applying the two-sample K–S test on $N_{re-samp} = 10^6$ number of resamples. The blue (green) PDF refers to the σ distribution corresponding to the original (post-processed) values of λ_{Edd} from the V21 simulation. The vertical blue and green dashed lines show the median of the blue and green distributions, respectively.

in the left panel of Fig. 1). Further, we applied the two-sample Kolmogorov–Smirnov (K–S) test (Kolmogorov 1933; Smirnov 1948) to the observed and simulated PDFs. We accounted for the uncertainties in the observed PDF by adopting the bootstrap re-sampling technique, as done in F22. To this aim, we first randomly re-sampled the observed PDF $N_{re-samp}$ times, taking into account the errors associated to the observational values. Then, we included the average error of the literature sample (∼0.1 dex, see Table 4 in F22 and Table 1 in M23) in the simulated PDF, and we randomly re-sampled it, as done for the observed one. Finally, for each $N_{re-samp}$ couple, we performed the two-sample K–S test, and we associated the corresponding σ values to the resulting p-values.

The right panel of Fig. 1 shows the PDF of the σ values resulting from the bootstrap re-sampling technique considering $N_{re-samp} = 10^6$. The median of the σ value PDF is 1.8. We found that the probability of having σ values greater than three is very small (∼1%), implying that the probability of rejecting the null hypothesis that these two samples are drawn from the same underlying distribution is not significant. We thus concluded that the simulated PDF provides a good representation of the observed one.

In the V21 simulation, however, the BH accretion is capped at the Eddington limit. To check whether and how much this assumption in the simulation affects the results, we used Eq. (1) to re-compute the accretion rate of the BHs for which $\lambda_{Edd} = 1$, and we repeated the K–S test analysis as detailed above. The resulting λ_{Edd} distribution from post processing is shown as a green shaded region in the left panel of Fig. 1; the K–S test results are shown in the right panel of the same figure with a green shaded region. The new median of the σ value PDF is 1.6 (instead of 1.8). The probability that we can reject the null hypothesis in this case is also ∼1%. This simple test suggests that our conclusions are not biased by the Eddington cap prescription on the accretion. We further discuss this caveat in Sect. 5.

To further validate our model, we compared the results of our simulation with the NIRSpec/PRISM sample by Greene et al. (2024), which contains seven AGN with $L_{bol} > 10^{44.2}$ erg s^{-1} within the redshift range $5.8 < z < 8.5$. For these sources, the estimated Eddington ratios range from 0.04 to 0.4. Such a range is consistent with the mean λ_{Edd} value (0.14) found in our simulation by applying the same luminosity cut in the redshift range $6 < z < 8.5$. Finally, we note that recent JWST spectroscopic observations of high-z ($7 < z < 10$) AGN (Bosman et al. 2023; Furtak et al. 2024; Kokorev et al. 2023) are consistent with sub-Eddington accretion rates ($\lambda_{Edd} \sim 0.3$–0.4), with the exception of CEERS_1019, whose accretion rate is consistent with the Eddington limit ($\lambda_{Edd} = 1.2 \pm 0.5$; Larson et al. 2023).

Table 1. Properties of the host galaxy of the most MBH in the simulation at $z = 10$ and GN-z11 (from Tacchella et al. 2023).

	SIM value	Observational value
log $M_*[M_\odot]$	8.9	$9.1^{+0.3}_{-0.4}$
SFR $[M_\odot\ \mathrm{yr}^{-1}]$	5.4	21^{+20}_{-10}

4. Eddington ratio predictions against $z \sim 10$ data

After confirming that the V21 model is able to reproduce the accretion properties of the well-studied population of $z \sim 6$ quasars, we searched in the simulation for BHs with $M_{BH} \sim 10^6\ M_\odot$ in the redshift range $10 < z < 11$ in order to investigate whether the same model can reproduce the properties of GN-z11 at $z = 10.6$. We found one BH-galaxy system in our simulated volume that can be representative of GN-z11. The BH seeded at $z \sim 16.1$ has a mass of $=1.4 \times 10^6\ M_\odot$ at $z = 10.6$, which is fairly consistent with the BH mass of GN-z11; however, it is accreting at $\lambda_{Edd} = 0.6$, smaller than what is suggested for GN-z11. We further report in Table 1 the properties of its host galaxy at $z = 10$, namely at the closest snapshot in our simulation to the GN-z11 redshift. The galaxy properties are consistent (within 1.6-σ) with those of GN-z11 in terms of both stellar mass (M_*) and SFR, as computed by Tacchella et al. (2023).

Furthermore, we computed the λ_{Edd} distribution of our GN-z11-like AGN with the same procedure adopted in Sect. 3, and we report the results in Fig. 2 with a shaded blue region. It is still possible that GN-z11 was detected while it was experiencing a rare episode of super-Eddington accretion. To compute the likelihood of this scenario, we relied on the EVS.

4.1. The extreme value statistics

We considered a cumulative distribution function (CDF), $F(x)$, and drew a sequence of N random variates $\{X_i\}$ from it. We called $X_{\max} \equiv \sup\{X_1 \dots X_N\}$ the largest value of this sequence. If all variables are identically distributed and mutually independent[5], then the probability that all of the deviates are less than or equal to some x is given by

$$\begin{aligned}\Phi(X_{\max} \leq x; N) &= F_1(X_1 \leq x) \dots F_N(X_N \leq x) \\ &= F^N(X).\end{aligned} \tag{4}$$

The PDF of $X_{\max}$ can then be obtained by differentiating Eq. (4) with respect to x:

$$\begin{aligned}\Phi(X_{\max} = x; N) &= N\, F'(x)[F(x)]^{N-1} \\ &= N\, f(x)[F(x)]^{N-1},\end{aligned} \tag{5}$$

where $f(x) = \mathrm{d}F(x)/\mathrm{d}x$ is the PDF of the considered distribution. Equation (5) provides the probability of finding the extreme value $X_{\max}$ after randomly extracting N variables from a given distribution f_x.

4.2. Application of the extreme value statistics to GN-z11

To apply the EVS to the case of GN-z11, we needed to know both (i) the functional form describing the PDF and CDF ($f(x)$ and $F(x)$, respectively, in Eq. (5)) of the simulated $\lambda_{\rm Edd}$ distribution and (ii) the number of random extractions (N in Eq. (5)) that apply to the case of JWST observations. For what concerns (i), we simply fit the blue shaded region in Fig. 2 with a Gaussian (solid blue line in Fig. 2), and we computed the corresponding CDF[6]. When fitting the simulated PDF with a Gaussian (solid blue line), the tail extends beyond the Eddington cap. Thus, even if the V21 simulations are capped at the Eddington limit, the probability of having extreme events, such as super-Eddington accretion episodes, is non-vanishing.

The calculation of (ii) was less trivial. We associated the number N of random extractions to the number of DM halos contained in the volume[7] V ($\sim 1.2 \times 10^6$ Mpc^3) covered by the observations (Oesch et al. 2016) that discovered GN-z11 in the CANDELS field. We thus adopted the following relation:

$$N = V \int_{m1}^{m2} \mathrm{d}M \left(\frac{\mathrm{d}n(M)}{\mathrm{d}M}\right)_{z=10.6}, \tag{6}$$

where m_1 and m_2 represent the minimum and maximum mass of the DM halo that are expected to host GN-z11 and $\frac{\mathrm{d}n(M)}{\mathrm{d}M}$ is the halo mass function, for which we considered the Sheth & Tormen (1999) functional form. We assumed $m_2 = 10^{13}\, M_\odot$ because we noticed that larger values do not change our results since the integral already converges with the assumed m_2 value. To estimate m_1, we adopted three different and independent approaches that rely on the SFR, M_*, and $M_{\rm BH}$ estimates of GN-z11 (see Appendix A). We derived that GN-z11 is hosted by a DM halo with a fiducial mass[8] of $M_{\rm h} \sim 0.7\text{–}4 \times 10^{11}\, M_\odot$. However, values as small as $M_{\rm h} \sim 4 \times 10^9\, M_\odot$ are not excluded by our analysis. We found $N = 0.006$, for $m_1 = 4 \times 10^{11}\, M_\odot$, that is, no DM halos of this mass are expected to be in the survey volume. Hence, we considered $7 \times 10^{10}\, M_\odot$ as the largest value for m_1 and $4 \times 10^9\, M_\odot$ as the smallest.

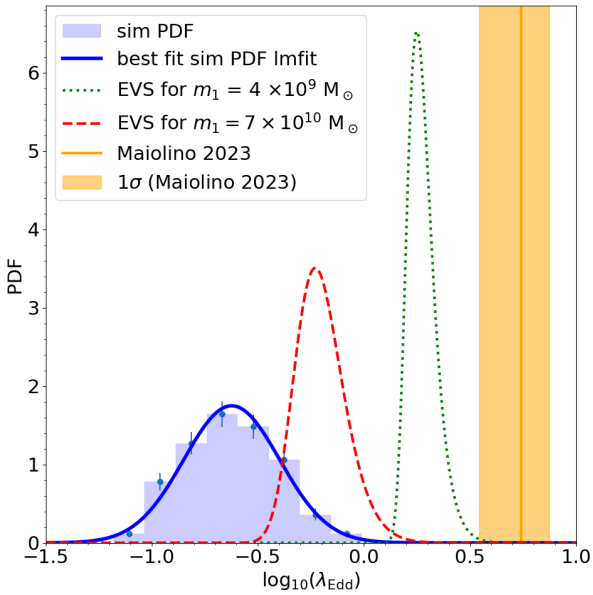

Fig. 2. Extreme value statistics PDF as a function of the Eddington ratio for a GN-z11-like AGN. Blue solid line shows the best-fit Gaussian (reduced $\chi^2_\nu = 1.4$) to the Eddington ratio distribution from the V21 simulation for BHs in the redshift range $10 < z < 11$ and $M_{\rm BH} > 10^6\, M_\odot$. The peak of the best fit is around $\lambda_{\rm Edd} \sim 0.25$. The dashed (dotted) red (green) line represents the EVS for the largest (smallest) considered value of m_1 (see text). The orange solid line (shaded region) shows the GN-z11 Eddington ratio (1σ uncertainty) estimated by Maiolino et al. (2024).

Figure 2 shows the EVS for the different values of m_1 mentioned above (see also Table 2). For the smallest value of m_1, namely the one providing the largest number of DM halos ($N = 16\,416$), $P(\lambda_{\rm Edd} > 1) = 0.98$ and $P(\lambda_{\rm Edd} > 3.5) = 2 \times 10^{-3}$. This means that our model allows for a non-vanishing probability of super-Eddington accretion episodes if $m_1 = 4 \times 10^9\, M_\odot$, but the probability of having $\lambda_{\rm Edd}$ values as large as the one observed in GN-z11 is very small in any case.

We repeated the same calculation of the accretion rate for the few ($\sim$2%) $\lambda_{\rm Edd} = 1$ episodes by removing the Eddington cap. We found that the results reported in Table 2 do not change. The maximum value of the Eddington ratio obtained in this case is $\lambda_{\rm Edd} = 2.24$. Such a value is smaller than that reported in Maiolino et al. (2024).

In summary, we quantified the probability that a GN-z11-like MBH, though accreting on average at $\lambda_{\rm Edd} = 0.25$, was detected while experiencing a rare episode of super-Eddington accretion. We find that this probability is very small ($<2 \times 10^{-3}$).

5. Summary and discussion

In this work, we have investigated the probability of having an MBH ($\sim 10^6\, M_\odot$) at $z \sim 10\text{–}11$ accreting at the super-Eddington rate ($\lambda_{\rm Edd} \sim 5.5$) similar to the one recently detected by JWST in

[5] We underscore that the hypothesis of independent accretion episodes is not satisfied in our approach since we are using the results obtained from a single zoom-in simulation. In Sect. 5, we further discuss this point and how we plan to overcome this limitation in future works.

[6] We adopt the python script `np.cumsum`

[7] A more recent estimate provides a smaller volume (2.2×10^5 Mpc^3; Naidu et al. 2022) than the one adopted here. A smaller volume would imply a smaller N value, thus strengthening the main result of our work.

[8] This estimate is consistent with the results by Scholtz et al. (2023) and Tacchella et al. (2023), according to which $M_{\rm h} \sim 3\text{–}8 \times 10^{10}\, M_\odot$.

Table 2. Extreme value statistics probability for $\lambda_{\rm Edd} > 1$ and >3.5 (namely the 1σ lower limit of the estimate by Maiolino et al. 2024 for GN-z11) resulting from different values of m_1 (see Eq. (6)).

m_1 [$M_\odot$]	N	$P(\lambda_{\rm Edd} > 1)$	$P(\lambda_{\rm Edd} > 3.5)$
4×10^9	16 416	0.98	2×10^{-3}
7×10^{10}	20	0.06	3×10^{-6}

GN-z11 (Maiolino et al. 2024). We first considered the accretion properties of simulated accreting SMBHs at $z \sim 6$–7.5 as provided by the zoom-in simulations developed by Valentini et al. (2021). By comparing the simulated $\lambda_{\rm Edd}$ PDF with the results from a state-of-the-art sample of $z \sim 6$ quasars (Farina et al. 2022; Mazzucchelli et al. 2023), we found that our accretion model successfully reproduces the data.

We then analysed the $\lambda_{\rm Edd}$ PDF of MBHs at $z \sim 10$–11 and computed the EVS. Assuming that the observations that discovered GN-z11 cover a volume of $\sim 1.2 \times 10^6$ Mpc^3 (Oesch et al. 2016), we find that the probability of finding a GN-z11-like object is very small ($\sim 10^{-3}$). Our result does not exclude the presence of an accreting MBH that is partly powering the GN-z11 luminosity. However, the BH-accretion and AGN-feedback recipes adopted in our model cannot reproduce the total observed luminosity of GN-z11. The discrepancy with JWST data suggests that the missing physics in our model (detailed below) have to boost the luminosities of $z \sim 10$ MBHs to the observed fluxes while still reproducing the $\lambda_{\rm Edd}$ PDF of $z \sim 6$ quasars.

One limitation of our work is that we are interpreting the super-Eddington accretion of GN-z11 with a model that caps the accretion to the Eddington limit. We justify this approximation with the fact that the V21 accretion model predicts that the probability of having maximal accretion ($\lambda_{\rm Edd} = 1$) is extremely small (~2%; see the blue distribution in Fig. 2). Thus, the assumption of the Eddington cap affects only a negligible number of accretion episodes. It is not straightforward to quantify the impact of the Eddington cap on the actual accretion rate. This is because feedback from super-Eddington episodes can greatly affect the surrounding medium, possibly quenching subsequent accretion events. Such an expectation is corroborated by the results in Massonneau et al. (2023, see Figs. 11 and 12). These authors compared the accretion rate evolution of MBHs as predicted by simulations with and without super-Eddington accretion and feedback. They found that models that account for super-Eddington accretion result in a smaller fraction of Eddington accretion episodes compared to the Eddington-capped case. This means that if the Eddington cap is removed in our simulation, the $\lambda_{\rm Edd}$ PDF would shift towards smaller values, thus yielding an even smaller EVS probability for $\lambda_{\rm Edd} > 1$.

If we consider the results from other studies allowing super-Eddington accretion rates onto BHs, the occurrence of $\lambda_{\rm Edd} \sim 5.5$ events is unlikely. To start with, in Massonneau et al. (2023), super-Eddington accretion events reach peak values of only two to three times the Eddington limit. Zhu et al. (2022) performed zoom-in hydrodynamical simulations of $z > 6$ SMBHs, exploring models with different seeding prescriptions, radiative efficiencies, accretion, and feedback models. In these simulations, the most extreme accretion event for MBHs is characterised by $\lambda_{\rm Edd} = 2.6$, and it only occurs at $z < 10$. Furthermore, in the radiation-hydrodynamic study by Pacucci & Ferrara (2015), the average Eddington ratio of the considered MBH is $\lambda_{\rm Edd} \sim 1.35$. The accretion halts when the emitted luminosity reaches the value $\sim 3\, L_{\rm Edd}$.

Finally, even state-of-the-art simulations (e.g. Lupi et al. 2023, but see also Jeon et al. 2024) that account for the entire range of accretion rates (from advection-dominated accretion flow to super-Eddington regimes) cannot explain the observational results of GN-z11. According to these calculations, $10^6\, M_\odot$ BH can experience super-Eddington accretion events (up to $\lambda_{\rm Edd} \sim 10$–100) when the MBH settles in the centre of the galaxy and the potential well becomes deep enough to sustain ingent gas inflows. This phase can be reached only after the supernova feedback stops perturbing the gas efficiently enough to hamper BH accretion. In this scenario, super-Eddington events only occur at $z < 9.5$, namely ~500 Myr after the MBH seeding.

Another caveat is that we have used results from a single zoom-in simulation. This is clearly insufficient to perform an extensive statistical analysis of the problem. In fact, when comparing the observed $\lambda_{\rm Edd}$ distribution with the simulation, we are considering a simulated MBH evolving from $10^8\, M_\odot$ at $z = 7.5$ to $10^9\, M_\odot$ at $z = 6$. In other words, we are making the strong assumption of associating different observed quasars to an accreting SMBH captured at different times during its accretion history.

Another assumption in our model that may affect the final results of our work concerns the seeding recipe. We have in fact considered only the possibility that SMBH can originate from heavy seeds (seed mass $\sim 10^5\, M_\odot$). It is not straightforward to foresee how this assumption might affect the simulated $\lambda_{\rm Edd}$ PDF and corresponding EVS. We can, however, mention that models considering the light seed scenario and allowing for super-Eddington accretion are unlikely to explain the extreme $\lambda_{\rm Edd}$ value found in GN-z11. For example, Smith et al. (2018) post processed the Renaissance simulation to follow the growth of BHs from individual remnants of Pop III stars, finding that (i) the accretion rate was very small ($<10^{-4}\, \lambda_{\rm Edd}$) for the majority of the ~15 000 BHs, (ii) only a small fraction (2–3%) of BHs accreted with $\lambda_{\rm Edd} > 10^{-4}$, and (iii) only one BH from ~15 000 BHs in a comoving volume of (40 Mpc)^3 accreted at the maximum accretion rate of $\lambda_{\rm Edd} \sim 3$, for a single timestep.

The robustness of the main conclusion of our work, namely the low probability of having a $10^6\, M_\odot$ super-Eddington accreting BH at $z \sim 10$, is weakened by the assumptions discussed above and the limitations of our approach. Still, our model proposes a novel method to link JWST observations with theoretical models in order to interpret, in particular, the overabundance of AGNs found at high-z (e.g. Maiolino et al. 2023; Harikane et al. 2023).

The most promising way to overcome the limitations of our work is to apply the EVS method to multiple large-scale simulations (e.g. Habouzit et al. 2021, 2022) that consider different seeding prescriptions and that also include light and intermediate seeds (Zhu et al. 2022). Furthermore, for a fair comparison with observed super-Eddington accretion events, it is important to properly model super-Eddington accretion in simulations adopting the radiatively inefficient slim-disc solution (Sądowski 2009). In this case, in fact, there is not a linear relation between $\lambda_{\rm Edd}$ and $\dot{M}_{\rm BH}/\dot{M}_{\rm Edd}$; in particular, the measured value of $\lambda_{\rm Edd}$ is expected to plateau at ~3 for $\dot{M}_{\rm BH}/\dot{M}_{\rm Edd} > 10$ (Madau et al. 2014).

From the observational point of view, further detections and characterisation of sources similar to GN-z11 in the early Universe will be fundamental to better constrain theoretical models and test their predictions against a larger data sample. In order to find rare sources, such as GN-z11, it is necessary to survey a $P(\lambda_{\rm Edd} > 3.5)^{-1} \sim 500\times$ larger volume with photometric

coverage at observed wavelengths greater than 1 μm and to then follow them up spectroscopically.

Acknowledgements. M.B. acknowledges support from PNRR funds. S.G. acknowledges support from the PRIN 2022 project (2022TKPB2P), titled: "BIG-*z*: Building the Giants: accretion, feedback and assembly in $z > 6$ quasars". M.V. is supported by the Fondazione ICSC National Recovery and Resilience Plan (PNRR), Project ID CN-00000013 "Italian Research Center on High-Performance Computing, Big Data and Quantum Computing" funded by MUR – Next Generation EU. M.V. also acknowledges partial financial support from the INFN Indark Grant. E.P.F. is supported by the international Gemini Observatory, a program of NSF's NOIRLab, which is managed by the Association of Universities for Research in Astronomy (AURA) under a cooperative agreement with the National Science Foundation, on behalf of the Gemini partnership of Argentina, Brazil, Canada, Chile, the Republic of Korea, and the United States of America.

References

Bañados, E., Venemans, B. P., Mazzucchelli, C., et al. 2018, Nature, 553, 473
Barkana, R., & Loeb, A. 2001, Phys. Rep., 349, 125
Bondi, H. 1952, MNRAS, 112, 195
Bondi, H., & Hoyle, F. 1944, MNRAS, 104, 273
Bosman, S. E. I., Álvarez-Márquez, J., Colina, L., et al. 2023, arXiv e-prints [arXiv:2307.14414]
Bouwens, R. J., Illingworth, G. D., González, V., et al. 2010, ApJ, 725, 1587
Bunker, A. J., Saxena, A., Cameron, A. J., et al. 2023, A&A, 677, A88
Chongchitnan, S., & Silk, J. 2012, Phys. Rev. D, 85, 063508
Chongchitnan, S., & Silk, J. 2021, Phys. Rev. D, 104, 083018
Coatman, L., Hewett, P. C., Banerji, M., et al. 2017, MNRAS, 465, 2120
Colombi, S., Davis, O., Devriendt, J., Prunet, S., & Silk, J. 2011, MNRAS, 414, 2436
Davis, O., Devriendt, J., Colombi, S., Silk, J., & Pichon, C. 2011, MNRAS, 413, 2087
Dayal, P., Ferrara, A., Dunlop, J. S., & Pacucci, F. 2014, MNRAS, 445, 2545
Decarli, R., Walter, F., Venemans, B. P., et al. 2018, ApJ, 854, 97
Decarli, R., Pensabene, A., Venemans, B., et al. 2022, A&A, 662, A60
Devecchi, B., Volonteri, M., Rossi, E. M., Colpi, M., & Portegies Zwart, S. 2012, MNRAS, 421, 1465
D'Odorico, V., Bañados, E., Becker, G. D., et al. 2023, MNRAS, 523, 1399
Eddington, A. S. 1926, The Internal Constitution of the Stars (Cambridge: Cambridge University Press)
Eisenstein, D. J., Willott, C., Alberts, S., et al. 2023, arXiv e-prints [arXiv:2306.02465]
Fan, X., Bañados, E., & Simcoe, R. A. 2023, ARA&A, 61, 373
Farina, E. P., Schindler, J.-T., Walter, F., et al. 2022, ApJ, 941, 106
Ferrara, A., Salvadori, S., Yue, B., & Schleicher, D. 2014, MNRAS, 443, 2410
Ferrara, A., Pallottini, A., & Dayal, P. 2023, MNRAS, 522, 3986
Furtak, L. J., Labbé, I., Zitrin, A., et al. 2024, Nature, 628, 8006
Gallerani, S., Fan, X., Maiolino, R., & Pacucci, F. 2017, PASA, 34, e022
Goulding, A. D., Greene, J. E., Setton, D. J., et al. 2023, ApJ, 955, L24
Greene, J. E., Strader, J., & Ho, L. C. 2020, ARA&A, 58, 257
Greene, J. E., Labbe, I., Goulding, A. D., et al. 2024, ApJ, 964, 39
Gumbel, E. J. 1958, Statistics of Extremes (New York: Columbia University Press)
Habouzit, M., Li, Y., Somerville, R. S., et al. 2021, MNRAS, 503, 1940
Habouzit, M., Somerville, R. S., Li, Y., et al. 2022, MNRAS, 509, 3015
Haehnelt, M. G., & Rees, M. J. 1993, MNRAS, 263, 168
Hahn, O., & Abel, T. 2011, MNRAS, 415, 2101
Harikane, Y., Zhang, Y., Nakajima, K., et al. 2023, ApJ, 959, 39
Harrison, I., & Coles, P. 2011, MNRAS, 418, L20
Hoyle, F., & Lyttleton, R. A. 1939, Proc. Camb. Philos. Soc., 35, 405
Inayoshi, K., Visbal, E., & Haiman, Z. 2020, ARA&A, 58, 27
Jeon, J., Bromm, V., Liu, B., & Finkelstein, S. L. 2024, ApJ, submitted [arXiv:2402.18773]
Kokorev, V., Fujimoto, S., Labbe, I., et al. 2023, ApJ, 957, L7
Kolmogorov, A. 1933, Inst. It. Attuari Giorn., 4, 83
Kotz, S., & Nadarajah, S. 2000, Extreme Value Distributions Theory and Applications (World Scientific)
Kroupa, P., Subr, L., Jerabkova, T., & Wang, L. 2020, MNRAS, 498, 5652
Krumholz, M. R. 2017, Star Formation (World Scientific Publishing Co.)
Larson, R. L., Finkelstein, S. L., Kocevski, D. D., et al. 2023, ApJ, 953, L29
Latif, M. A., & Ferrara, A. 2016, PASA, 33, e051
Le Fèvre, O., Lemaux, B. C., Nakajima, K., et al. 2019, A&A, 625, A51
Lovell, C. C., Harrison, I., Harikane, Y., Tacchella, S., & Wilkins, S. M. 2023, MNRAS, 518, 2511
Lupi, A., Haardt, F., Dotti, M., et al. 2016, MNRAS, 456, 2993
Lupi, A., Quadri, G., Volonteri, M., Colpi, M., & Regan, J. A. 2023, A&A, in press https://doi.org/10.1051/0004-6361/202348788
Madau, P., & Rees, M. J. 2001, ApJ, 551, L27
Madau, P., Haardt, F., & Dotti, M. 2014, ApJ, 784, L38
Maiolino, R., Scholtz, J., Curtis-Lake, E., et al. 2023, A&A, submitted [arXiv:2308.01230]
Maiolino, R., Scholtz, J., Witstok, J., et al. 2024, Nature, 627, 59
Massonneau, W., Volonteri, M., Dubois, Y., & Beckmann, R. S. 2023, A&A, 670, A180
Mayer, L., & Bonoli, S. 2019, Rep. Progr. Phys., 82, 016901
Mazzucchelli, C., Bischetti, M., D'Odorico, V., et al. 2023, A&A, 676, A71
Mikelsons, G., Silk, J., & Zuntz, J. 2009, MNRAS, 400, 898
Naidu, R. P., Oesch, P. A., van Dokkum, P., et al. 2022, ApJ, 940, L14
Oesch, P. A., Brammer, G., van Dokkum, P. G., et al. 2016, ApJ, 819, 129
Orofino, M. C., Ferrara, A., & Gallerani, S. 2018, MNRAS, 480, 681
Pacucci, F., & Ferrara, A. 2015, MNRAS, 448, 104
Pacucci, F., Natarajan, P., Volonteri, M., Cappelluti, N., & Urry, C. M. 2017, ApJ, 850, L42
Pacucci, F., Nguyen, B., Carniani, S., Maiolino, R., & Fan, X. 2023, ApJ, 957, L3
Pensabene, A., Carniani, S., Perna, M., et al. 2020, A&A, 637, A84
Pezzulli, E., Valiante, R., & Schneider, R. 2016, MNRAS, 458, 3047
Pezzulli, E., Volonteri, M., Schneider, R., & Valiante, R. 2017, MNRAS, 471, 589
Planck Collaboration VI. 2020, A&A, 641, A6
Reines, A. E., & Volonteri, M. 2015, ApJ, 813, 82
Richards, G. T., Haiman, Z., Pindor, B., et al. 2006, AJ, 131, 49
Rodríguez Hidalgo, P. 2009, PhD Thesis, University of Florida, USA
Schneider, R., Valiante, R., Trinca, A., et al. 2023, MNRAS, 526, 3250
Scholtz, J., Witten, C., Laporte, N., et al. 2023, A&A, submitted [arXiv:2306.09142]
Shen, Y., & Liu, X. 2012, ApJ, 753, 125
Shen, Y., Richards, G. T., Strauss, M. A., et al. 2011, ApJS, 194, 45
Sheth, R. K., & Tormen, G. 1999, MNRAS, 308, 119
Sądowski, A. 2009, ApJS, 183, 171
Sądowski, A., & Gaspari, M. 2017, MNRAS, 468, 1398
Smirnov, N. 1948, Ann. Math. Stat., 19, 279
Smith, B. D., Regan, J. A., Downes, T. P., et al. 2018, MNRAS, 480, 3762
Springel, V. 2005, MNRAS, 364, 1105
Tacchella, S., Eisenstein, D. J., Hainline, K., et al. 2023, ApJ, 952, 74
Terao, K., Nagao, T., Onishi, K., et al. 2022, ApJ, 929, 51
Trakhtenbrot, B., & Netzer, H. 2012, MNRAS, 427, 3081
Trinca, A., Schneider, R., Valiante, R., et al. 2022, MNRAS, 511, 616
Trinca, A., Schneider, R., Valiante, R., et al. 2024, MNRAS, 529, 3563
Valentini, M., Murante, G., Borgani, S., et al. 2017, MNRAS, 470, 3167
Valentini, M., Borgani, S., Bressan, A., et al. 2019, MNRAS, 485, 1384
Valentini, M., Murante, G., Borgani, S., et al. 2020, MNRAS, 491, 2779
Valentini, M., Gallerani, S., & Ferrara, A. 2021, MNRAS, 507, 1
Venemans, B. P., Walter, F., Decarli, R., et al. 2017, ApJ, 851, L8
Venemans, B. P., Walter, F., Neeleman, M., et al. 2020, ApJ, 904, 130
Vestergaard, M., & Osmer, P. S. 2009, ApJ, 699, 800
Vestergaard, M., & Peterson, B. M. 2006, ApJ, 641, 689
Volonteri, M., & Bellovary, J. 2012, Rep. Progr. Phys., 75, 124901
Volonteri, M., Habouzit, M., & Colpi, M. 2021, Nat. Rev. Phys., 3, 732
Waizmann, J. C., Ettori, S., & Moscardini, L. 2011, MNRAS, 418, 456
Wang, R., Wu, X.-B., Neri, R., et al. 2016, ApJ, 830, 53
Wang, F., Fan, X., Yang, J., et al. 2021, ApJ, 908, 53
Yang, J., Wang, F., Fan, X., et al. 2020, ApJ, 897, L14
Yang, J., Wang, F., Fan, X., et al. 2023, ApJ, 951, L5
Zhu, Q., Li, Y., Li, Y., et al. 2022, MNRAS, 514, 5583

Appendix A: Halo mass estimation for GN-z11

In this Appendix, we compute the range of the allowed masses for the DM halos that host GN-z11, based on the SFR and M_* estimates, and considering different $M_{\rm BH} - M_*$ relations. We find that the fiducial value corresponds to $M_{\rm h} = 4 \times 10^{11}\,{\rm M}_\odot$.

A.1. Halo mass estimation from the star formation rate

To estimate the halo mass M_h from the SFR, we adopted the relation proposed by Ferrara et al. (2023),

$$\mathrm{SFR} = 22.7 \left(\frac{\epsilon_{\rm SF}}{0.01}\right) \left(\frac{1+z}{8}\right)^{3/2} \left(\frac{M_{\rm h}}{10^{12}\,{\rm M}_\odot}\right) {\rm M}_\odot\ {\rm yr}^{-1} \tag{A.1}$$

where $\epsilon_{\rm SF}$ is star formation efficiency that depends on the supernova (SN) feedback as in Dayal et al. (2014):

$$\epsilon_{\rm SF} = \epsilon_0\ \frac{v_c^2}{v_c^2 + f_w\ v_s^2}, \tag{A.2}$$

where $f_w = 0.1$ is the coupling efficiency of SN energy with gas, $v_c(M)$ is the halo circular velocity (e.g. Barkana & Loeb 2001), ϵ_0 is fixed to 0.02 to be consistent with local galaxy measurements (Krumholz 2017), $v_s = \sqrt{\nu\ E_0}$ is the characteristic velocity corresponding to the SN energy (E_0) released per unit stellar mass. Considering $E_0 = 10^{51}$ erg and $\nu^{-1} = 52.89\,{\rm M}_\odot$ same as in Ferrara et al. (2023), we get $v_s = 975\,{\rm km\,s^{-1}}$.

The SFR of GN-z11 derived from the NIRCam photometry (assuming no contribution from the AGN) is $\mathrm{SFR} = 21^{+22}_{-10}\,{\rm M}_\odot\,{\rm yr}^{-1}$ (Tacchella et al. 2023). This corresponds to $M_{\rm h} = 4 \times 10^{11}\,{\rm M}_\odot$. By considering the 2 σ deviation, we end up with the following possible range of halo mass: $5{\times}10^{10} < (M_{\rm h}/{\rm M}_\odot) < 1 \times 10^{12}$.

A.2. Halo mass estimation from the stellar mass

Stellar mass M_* can be related to halo mass $M_{\rm h}$ using the following relation:

$$M_{\rm h} = \frac{\Omega_{\rm dm}}{\Omega_{\rm b}} \left(\frac{M_*}{\epsilon_*}\right), \tag{A.3}$$

where $\epsilon_* = 0.1$ is the conversion efficiency of baryons to stars. The stellar mass of GN-z11 derived from the NIRCam photometry is $\log_{10}(M_*/{\rm M}_\odot) = 9.1^{+0.3}_{-0.4}$ (Tacchella et al. 2023). This corresponds to $M_{\rm h} = 7 \times 10^{10}\,{\rm M}_\odot$. By considering the 3σ deviation, we ended up with the following possible range of halo mass: $4 \times 10^9 < (M_{\rm h}/{\rm M}_\odot) < 5 \times 10^{11}$.

A.3. Halo mass estimation from the black hole mass

In the local Universe, BH mass scales with stellar mass as $M_{\rm BH} \sim 10^{-4}\,M_*$ (Reines & Volonteri 2015). However, it has been found that high-z SMBHs can be overmassive with respect to their low-z counterparts by a factor greater than ten (Pensabene et al. 2020; Pacucci et al. 2023). In particular, Pacucci et al. (2023) suggest the following relation for the high z: $M_{\rm BH} \sim 10^{-2}\,M_*$. By combining the local and high-z relations with Eq. A.3 and assuming $M_{\rm BH} = 1.6 \times 10^6\,{\rm M}_\odot$ (Maiolino et al. 2024), we estimate that GN-z11 should be hosted by a DM halo of mass $9 \times 10^9 < (M_{\rm h}/{\rm M}_\odot) < 9 \times 10^{11}$.